Ultrasonics Sonochemistry 111 (2024) 107110

Contents lists available at ScienceDirect

Ultrasonics Sonochemistry

journal homepage: www.elsevier.com/locate/ultson

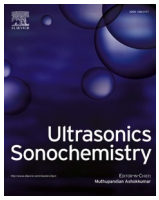

Proof-of-concept for removing micropollutants through a combination of sub-atmospheric-pressure non-thermal plasma and hydrodynamic (super) cavitation

Mojca Zupanc [a], Gregor Primc [b,*], Matevž Dular [a], Martin Petkovšek [a], Robert Roškar [c], Rok Zaplotnik [b], Jurij Trontelj [c,*]

[a] Faculty of Mechanical Engineering, University of Ljubljana, Aškerčeva cesta 6, 1000 Ljubljana, Slovenia
[b] Department of Surface Engineering, Jožef Stefan Institute, Jamova cesta 39, 1000 Ljubljana, Slovenia
[c] Faculty of Pharmacy, University of Ljubljana, Aškerčeva cesta 7, 1000 Ljubljana, Slovenia

ARTICLE INFO

Keywords:
Water treatment
Gaseous plasma
Oxidation
Pharmaceuticals
Endocrine-disrupting chemicals
(Super)cavitation

ABSTRACT

The persistence and toxicity of hazardous pollutants present in wastewater effluents require the development of efficient and sustainable treatment methods to protect water resources. In this study, the efficacy and efficiency of a novel combination of two advanced oxidation processes – sub-atmospheric-pressure plasma and hydrodynamic cavitation – were systematically tested for the removal of valsartan (VAL), sulfamethoxazole, trimethoprim, naproxen, diclofenac (DF), tramadol, propyphenazone, carbamazepine, 17β-estradiol (E2) and bisphenol A (BPA). The results show that both sample temperature and plasma power play a role and the highest removal, from 29–99 %, was achieved at 25 °C and 53 W of plasma power. E2, BPA, DF, and VAL were removed to the highest degree. These results are particularly important in the case of E2 and BPA, whose harmful environmental effects may start to occur already at sub-ng/L to μg/L levels. The differences in the removals obtained depend strongly on the physicochemical properties, and the compounds with the highest logK_{OW} were removed to the highest extent. The energy yield, in terms of plasma power, was between 1 and 26 mg/kWh under optimal experimental conditions. Our results show that the novel plasma-cavitation treatment shows potential that could prove valuable for upcoming regulatory requirements.

1. Introduction

The number of publications documenting the presence of pharmaceuticals and endocrine-disrupting chemicals (EDCs) in concentrations ranging from ng/L to μg/L in water bodies worldwide continues to increase [1–7]. In addition, there is growing evidence of their potentially harmful effects on non-target organisms, including humans [8,9] and in the case of EDCs, even at concentrations of a few ng/L [8,10,11]. However, conventional water treatment methods often prove inadequate to address the intricate nature of these pollutants effectively, making wastewater treatment plants (WWTPs) a major source through which these compounds enter the aquatic environment [10,12,13]. In response to growing concerns about water pollution and to ensure water quality across the EU, a Watch list of priority substances to be monitored in EU surface waters has been established within the Water Framework Directive (WFD) [14]. Accumulating evidence of the negative impacts of these substances has finally led to legislative action, with forthcoming EU legislation [15] recommending quaternary treatment to remove micropollutants from wastewater (WW), where ≥ 80 % of the targeted pollutants will have to be removed.

The development of effective and sustainable alternative water treatment technologies that could be retrofitted in conventional WWTPs

Abbreviations: AOP, advanced oxidation process; BPA, bisphenol A; CBZ, carbamazepine; DBD, dielectric barrier discharges; DF, diclofenac; E2, 17β-estradiol; EDC, endocrine-disrupting chemicals; HC, hydrodynamic cavitation; G, energy yield; JET, plasma jets and torches; LLOQ, lower limit of quantification; MRM, multiple reaction monitoring; NP, naproxen; PCD, pulsed corona discharges; PPZ, propyphenazone; PSD, pulsed spark discharges; RGHC, rotational generator of hydrodynamic cavitation; SFX, sulfamethoxazole; TMD, tramadol; TMP, trimethoprim; VAL, valsartan; WFD, Water Framework Directive; WW, wastewater; WWT, wastewater treatment; WWTP, wastewater treatment plant.

* Corresponding authors.
E-mail address: jurij.trontelj@ffa.uni-lj.si (J. Trontelj).

https://doi.org/10.1016/j.ultsonch.2024.107110
Received 9 August 2024; Received in revised form 8 October 2024; Accepted 14 October 2024
Available online 16 October 2024

is therefore more urgent than ever. Over the years, sufficient data have been collected to confirm that $^{\bullet}OH$ generated in advanced oxidation processes (AOPs) such as Fenton oxidation, electrochemical oxidation, photocatalysis, cavitation, gaseous plasmas (hereinafter: plasmas), and UV/H_2O_2, indiscriminately attack many structurally diverse hazardous organic pollutants, leading to their partial or complete oxidation [16–18]. Two promising AOPs that have been extensively studied in recent years, either individually or in combination, are cavitation and atmospheric-pressure plasma. Cavitation is a phenomenon of rapid evaporation and condensation in which small vapor bubbles form in a liquid due to a local pressure drop. When the formed bubbles collapse, the energy captured inside is transformed into a very small spatio-temporal region, triggering mechanical and chemical effects associated with cavitation [19]. The effectiveness of hydrodynamic cavitation (HC) as a water treatment process has been critically evaluated in numerous review papers in recent years [16,20,21]. Even though commonly studied mechanisms of HC generation include static devices such as orifices and venturi constrictions [16,22,23] and dynamic devices such as rotational generators of HC (RGHCs) [16,24,25], the degradation of various micropollutants is most studied on the former. To intensify these processes and achieve synergistic effects, cavitation is often combined with external oxidants [16,22,24,26]. In HC, typical cavitation regimes can be distinguished between incipient cavitation, sheet (attached) cavitation, developed (cloud shedding) cavitation, and finally, supercavitation, when the static pressure drops sharply in a larger spatio-temporal region, which usually appears as a large single stable cavitation bubble extending beyond the trailing edge of the hydrofoil or other constrictions [27]. Similarly, atmospheric-pressure plasmas have been extensively studied for the removal of various micropollutants [2,7,8], where their degradation occurs either through their direct interaction with UV radiation or reactive oxygen and nitrogen species such as O_3, $^{\bullet}OH$, $HO_2^{\bullet}$, $^1O_2$, $O_2^{\bullet-}$, H_2O_2, NO^{3-}, NO^{2-}, NO and $ONOO^-$ [28,29]. Since plasma can only be ignited in gases, the path of the plasma-generated species (atoms, ions, radicals, photons, excited molecules, and atoms) into the water sample is an important factor. This path depends on the plasma setup, and many different setups have already been studied (Table 4). They include devices where plasma is ignited either far away from the water surface [6,30,31], close to the water surface [7,32], or in the water with the help of bubbles [2]. Additionally, plasma species can be formed remotely and bubbled into the liquid [6]. The difference between these methods and the use of different gases lies in the generated reactive oxygen and nitrogen species and their diffusivity into the water; the latter are only present when air (or a mixture with nitrogen) is used as the discharge gas [33]. Plasmas generated above water or in a gas bubble can be generated using various plasma types: pulsed corona discharges (PCD) [2–4,7,28,34,35], dielectric barrier discharges (DBD), or even pulsed spark discharges (PSD) [5,11,31,32,36–39] and plasma jets and torches (JET) [29,30] (Table 4). Some plasma systems operate in batch mode [31], while others operate in flow-through mode [7].

The problem with AOPs, however, is that they all have their weaknesses, and no single process can cover everything: be simple, environmentally friendly, without secondary pollution, economically feasible, robust, and easily scalable. One of the disadvantages of HC is that $^{\bullet}OH$ are formed at the gas–liquid interface, which reduces its effectiveness in treating micropollutants with a $\log K_{ow} < 3.5$ [40], as they do not reach the sites where $^{\bullet}OH$ are formed, which is why external oxidizing agents are often used to intensify the process. Likewise, for different types of atmospheric-pressure plasmas, the transport efficiency of the short-lived reactive species from the gas to the liquid bulk phase is also one of the major drawbacks [6,41]. The disadvantage is that the density of the reactive species decreases rapidly with distance. This is due to the three-body collisions, which are very frequent at atmospheric pressure (about 10^7 s^{-1}), while the frequency of three-body collisions is 1,000 times lower at about 30 mbar (of absolute pressure). For this reason, certain reactive species that can react with and degrade the studied compounds do not reach them, limiting the full potential of the process and hindering its use on an industrial scale. Some authors have already addressed this transfer problem by increasing the interface between the gas and the liquid phase by introducing plasma bubbles from the outside into the water sample under investigation [2,41,42]. Another distinguishing feature of plasmas is the formation of long-lived reactive species, such as H_2O_2, the concentration of which increases with prolonged continuous treatment time [2,28,30,38]. Thus, a possible solution to address these shortcomings could lie in the combination of two or more processes that complement each other and in which one process can enhance the other, like HC and plasma. Such a combination could reduce environmental impact and increase the overall effectiveness and efficiency. Several research groups have already attempted to combine HC and atmospheric-pressure plasma to increase treatment efficiency [43–46], but studies investigating novel combination options and testing their effectiveness on a mixture of different micropollutants are still lacking. For example, the existing studies mainly investigate atmospheric-pressure plasma, while there are hardly any studies investigating the effects of sub-atmospheric-pressure plasmas [45]. Furthermore, different plasmas, including sub-atmospheric-pressure plasma and RGHC, have not been combined yet, and investigations on how to further exploit the H_2O_2 generated during plasma operation are also lacking.

For this reason, the main objectives of this study were:

(i) to serially couple sub-atmospheric-pressure non-thermal plasma ignited in the supercavitation bubble formed in the Venturi constriction with a laboratory-scale RGHC (SupCaviPlasma device) and evaluate reactive species generated (Fig. 1);
(ii) to determine the removal, degradation kinetics, and degradation half-life times ($t_{1/2}$) of structurally different micropollutants in the novel SupCaviPlasma device under different experimental conditions (for the first time in the case of propyphenazone);
(iii) to test the hypothesis of whether H_2O_2 formed during plasma could be further exploited in the RGHC; and
(iv) to compare the efficiency of the novel SupCaviPlasma device with other available plasma types.

The compounds selected for this study have different physico-chemical properties and belong to different groups of emerging micropollutants. These include the pharmaceuticals angiotensin II receptor blocker valsartan (VAL), two antibacterial agents for systemic use, sulfamethoxazole (SFX) and trimethoprim (TMP), two non-steroidal anti-inflammatory drugs naproxen (NP) and diclofenac (DF), the opioid tramadol (TMD), the analgesic and antipyretic propyphenazone (PPZ), the antiepileptic carbamazepine (CBZ) and two EDCs, the estrogen 17β-estradiol (E2) and an industrial chemical bisphenol A (BPA). These structurally different micropollutants were selected because of their presence in WWTP effluents, resistance to biological degradation, increasing occurrence in the future and because the data on their harmful effects on aquatic ecosystems are extensive [9]. This is also confirmed by the fact that SFX, TMP, DF, and E2 are currently or have been in the past included on the WFD's Watch list of priority substances. The chemical structures and some physico-chemical properties of the selected micropollutants can be found in Supplementary Material, Suppl. 1.

2. Materials and methods

2.1. Standards and chemicals

Analytical standards used for the experiments and the development and calibration of the analytical method were of high purity grade (> 99 %): valsartan, sulfamethoxazole, trimethoprim, naproxen, diclofenac sodium, carbamazepine, propyphenazone, bisphenol A and tramadol were purchased from Sigma-Aldrich (Steinheim, Germany), while 17β-

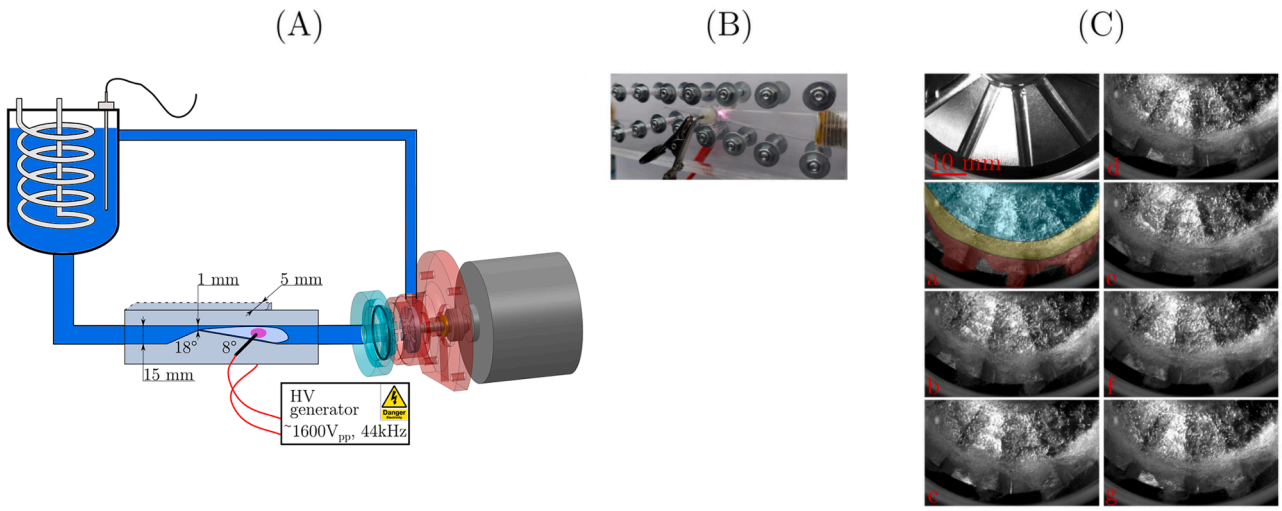

Fig. 1. (A) Schematic presentation of the plasma-cavitation treatment in the SupCaviPlasma setup; (B) Image of plasma formation in Venturi constriction; (C) cavitation visualization within the RGHC.

estradiol was purchased from Carbosynth (Berkshire, United Kingdom). The potassium iodide was of analytical grade and supplied by Merck (Darmstadt, Germany).

2.2. Instrumental analysis

2.2.1. LC-MS method for the determination of a mix of micropollutants in plasma-cavitation experiments

The treated samples were analyzed by a UHPLC 1290 Infinity II (Agilent, Santa Clara, USA) coupled to a triple quadrupole/hybrid ion trap mass spectrometer 5500 Qtrap (Sciex, Ontario, Canada). Briefly, 10 µL samples were injected onto a Poroshell 50 mm × 2.1 mm, 1.8 µm C18 column maintained at 50 °C. The analytes were eluted by a mobile phase A 0.025 % acetic acid in MilliQ water and mobile phase B methanol with a linear gradient with the following time and %B content points: (0 min, 8 %), (1 min, 10 %), (2 min, 30 %), (5 min, 50 %), (8 min, 8 %). The analytes were quantified in multiple reaction monitoring (MRM) mode (Suppl. 2, Table S2a). The method's calibrated working range was established at least from 1 µg/L to 100 µg/L, in some cases even from 0.25 µg/L to 100 µg/L based on accuracy (85–115 %), precision (RSD < 15 %), and signal-to-noise ratio: S/N > 10, except at lower limit of quantification (LLOQ), where the accuracy and precision were 80–120 %, and RSD 20 %, or better, respectively (Suppl. 2, Table S2b). Three quality control samples were prepared from separate standard weighing and checked for accuracy and precision (at 10, 50, and 100 µg/L) in each analytical run. Method details and performance data can be found in Suppl. 2, Fig. 2Sa and 2Sb.

2.3. Experimental device

2.3.1. SuperCavitation plasma setup – SupCaviPlasma

The experimental setup (Fig. 1 (A)) consisted of a Venturi constriction (1) where a supercavitation bubble can form coupled to the RGHC reactor (2) and a 5 L reservoir (3) in a closed circuit. RGHC reactor with

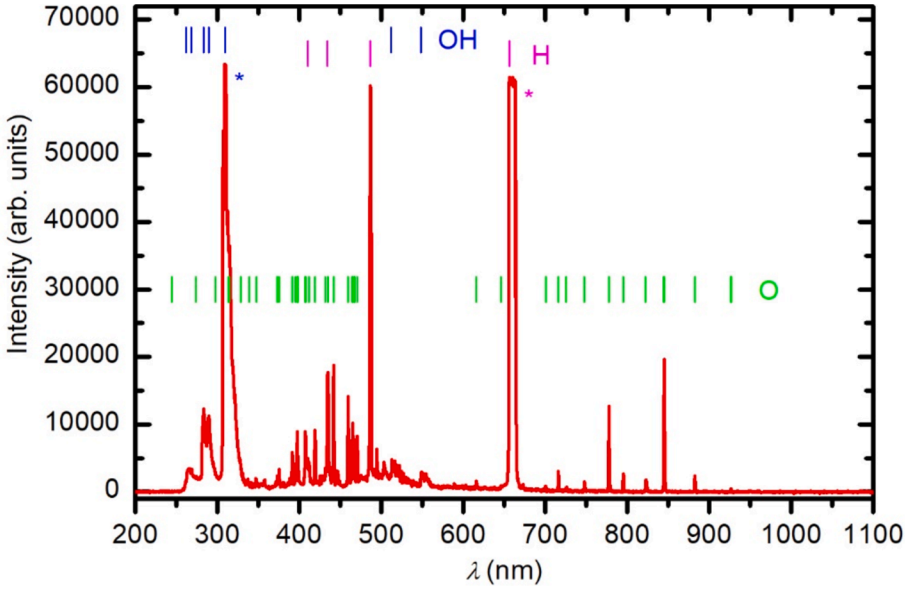

Fig. 2. Optical emission spectra of the plasma inside the supercavitation bubble. The asterisk denotes the saturation of the spectral feature (signal beyond the maximum capability of the CCD detector). Vertical color lines or marks denote which spectral feature belongs to which atoms or molecules (green denotes oxygen atoms, magenta denotes hydrogen atoms, and blue denotes OH molecules). (For interpretation of the references to color in this figure legend, the reader is referred to the web version of this article.)

its double function (cavitation generator and pumping performance) was used to establish the supercavitation bubble in the Venturi nozzle and simultaneously generate developed cavitation inside the RGHC chamber. A stable supercavitation bubble was needed to ignite the gaseous plasma. Downstream, the RGHC improves the mass transfer from the gas to liquid phase by scattering and mixing the short- and long-lived reactive species formed by plasma (e.g., $^{\bullet}OH$, H_2O_2), by cavitation formed in the RGHC (mainly $^{\bullet}OH$) and potentially also by small cavities shed from the closure region of the supercavitation bubble [47]. The Idea of coupling RGHC in the setup was also to exploit H_2O_2 formed during plasma operation for improving the oxidative potential of developed cavitation. Since the purpose of the present study was to confirm whether and to what extent selected micropollutants can be removed with the sole combination of sub-atmospheric plasma formed inside the stable supercavitation bubble and developed cavitation (formed inside the RGHC), no partial control experiments were performed with separate contributions from the plasma generated in the supercavitation bubble, and $^{\bullet}OH$ produced due to the cloud shedding of supercavitation bubble or developed hydrodynamic cavitation in the RGHC. In continuation, the synergistic effect of plasma formed inside the supercavitation bubble in the Venturi part (shown in the manuscript in Fig. 1 A(1) and B), shedding of the supercavitation cloud (Fig. 1 (1)) and the developed cavitation inside the RGHC (shown in the manuscript in Fig. 1 A (2) and C) is referred to as the SupCaviPlasma device.

Sub-atmospheric-pressure non-thermal plasma (shown in Fig. 1 (B)) (hereinafter simply named plasma) was generated in the divergent part of the Venturi nozzle (constriction with convergent-divergent angle of 18° and 8° respectively and cross-section of 1 mm × 5 mm at the throat) between two electrodes that penetrated the supercavitation bubble. The two electrodes were made from stainless-steel rods that were firmly enclosed in glass tubes to prevent the metal from coming into direct contact with liquid water. The bare part of the electrode was only at the tip, which was in the gas bubble. This detailed description of the device can also be found in the US patent (US11807555B2), which was granted in October 2023 [48]. A sinusoidal high-frequency generator (Fig. 1 (4)) (ZVS driver, High Voltage Shop, Austria) operating at 44 kHz was connected to the electrodes. High-frequency generator was powered by a DC voltage power supply. Three different DC voltages were used for powering the high-frequency generator: 12, 18, and 24 V (resulting in power consumptions given in Table 1), with the peak-to-peak voltage between the electrodes being 1,630, 1,670, and 1,680 V, respectively. The rotor–stator geometry in the RGHC comprised a 12-tooth rotor with teeth inclination of 10.7° and 70 mm in diameter, which was combined with a flat surface stator with a 4 mm gap between them. The rotational frequency of the rotor was set to 9,000 rpm, which equalled 33 m/s of circumferential velocity at the outermost diameter of the rotor. The sample temperature was monitored using a commercial 4-wire RTD Pt100 thermometer (Class A) installed directly in the reservoir. It was maintained via a cooling coil connected to the Polyscience DuraChill (PolyScience, USA) external portable cooling unit with a cooling capacity of 1.28 kW. The flow rate for selected experimental conditions was evaluated using the volumetric method. Fig. 1 (C) shows cavitation visualization within the RGHC chamber with a time step of 0.156 ms. Three distinct regions can be observed: (i) inner circle with low velocity and low-pressure region, which results in a high volume fraction of large bubbles (highlighted with cyan), (ii) transition ring where the pressure and velocity are higher what leads to the presence of numerous small cavitation bubbles forming white appearance (highlighted with yellow), and (iii) the outer rotor's region with the highest pressure and velocity that lead to developed cavitation with cloud shedding (highlighted with red).

Table 1
Investigated experimental conditions.

Exp.	T (°C)	Treatment time (min)	U_{PL} (V)	P_{PL} (W)	P_{RGHC} (W)	Q (L/min)
A	25	1, 2, 3, 4, 5, 10, 20, 30	12	25	530	4.9
B			18	36	530	4.9
C			24	53	530	4.9
D	15		24	52	530	4.9
E	40		24	55	440	4.9
F	60		24	61	340	4.3

P_{PL}: plasma excitation power measured under the investigated experimental conditions; P_{RGHC}: power measured for RGHC under the investigated experimental conditions; Q: measured flow rate with uncertainty of ± 0.1 L/min.

2.3.2. Plasma and cavitation characterization

Plasma was characterized with optical emission spectroscopy. An optical fiber was carefully inserted into the supercavitation bubble near the plasma without disturbing the water flow or integrity of the bubble. AvaSpec 36,448 fiber optic spectrometer (Avantes, Netherlands) with 0.3 nm resolution from 200 to 1,200 nm with an integration time of 2 s was used.

Developed cavitation in the RGHC was characterized by high-speed visualization (Fig. 1 (C)). Visualization was performed with a high-speed camera Photron FastCam Mini UX 100 at 6,400 fps and resolution of 1,280 × 776 pixels in 12-bit monochrome mode. By using high-power LED illumination, we were able to lower the shutter time down to 5 μs. Energy consumption of each, plasma and RGHC, during the investigated experimental conditions (Table 1), was measured using a Norma 4,000 Power Analyzer (Fluke, Netherlands).

The degradation effectiveness and efficiency evaluation of the SupCaviPlasma was performed via calculations of removals (%), degradation kinetics, and energy yields (G). For plasma and RGHC, two separate G-values (G_{PL} and $G_{PL+RGHC}$) (mg/kWh) were calculated. The calculation of the G-values was based on [2] and corresponded to 90 % of the micropollutant removal (Eq. (1):

$$G_{90}(mg/kWh) = \frac{0.9C_0V}{Pt} \quad (1)$$

where C_0 (mg/L) is the initial concentration of the micropollutants, V (L) is the volume of the treated sample, P (kW) is the power needed for the removal of 90 % of micropollutant, and t (h) is the time, required for 90 % removal of micropollutants. Due to easier comparison with the results from the literature, also G_{50}, G_{60} and G_{100} values, which correspond to 50, 60 and 100 % of the micropollutants removal, were calculated (Table 4). In addition to G-values also EEO-values (electrical energy per order) were calculated and are only presented in Suppl. 8.

2.4. Experimental conditions and design

The overview of the experiments (Exps. A−F) performed for the evaluation of the removal of selected micropollutants in the novel SupCaviPlasma device is presented in Table 1. The effects of plasma excitation power (P_{PL}) and recirculating water temperature (T) were varied to determine which one and to what extent influenced the removal of the compounds. Experiments were conducted in 3 L MilliQ water samples, each sample containing all 10 micropollutants with a fixed concentration (100 μg/L of each). The micropollutant standards were prepared in methanol, and when added to 3 L of MilliQ water, the final concentration of methanol was 0.01 %. Before and after each investigated treatment time (1, 2, 3, 4, 5, 10, 20, and 30 min), 1 mL of samples was taken for the determination of the remaining compounds by LC-MS analysis. Potassium iodide was added to the 1 mL samples (20 μL of 1 mg/mL standard solution) to quench residual reactive species after plasma-cavitation treatment. After each experiment, the SupCaviPlasma device was cleaned with 3 L of MilliQ water to prevent any possible contamination of samples. After the first cleaning cycle, another blank treatment with pure MilliQ water was performed, and the water was sampled for any residual micropollutants. The results confirmed this

cleaning protocol as satisfactory.

In addition to LC-MS measurements, H_2O_2, dissolved O_2, and pH were measured before experiments, and after 5, 10, 20, and 30 min of treatment H_2O_2 was measured using a Photometer (7500 BT, Palintest, UK), whereas O_2 and pH were measured using a multimeter HQ430d with LD0101 and PHC725 probes (Hach, USA), respectively. For these measurements, 50 mL samples were taken each time. The results of these measurements are given in Suppl. 3.

To confirm that the observed removals of selected micropollutants during the combined plasma-cavitation treatment occur primarily due to the short-lived species (e.g. $^{\bullet}OH$) and not the long-lived ones (e.g. H_2O_2), two additional experiments (Exps. G and H) were performed (Table 2). Here, only MilliQ water without micropollutants was first treated with the SupCaviPlasma device under the experimental conditions given in Table 2 (Exp. G), and a mix of investigated micropollutants (100 μg/L of each) was added into the solution after 45 min of plasma-cavitation treatment. Afterwards, this solution was put on the magnetic stirrer for an additional 30 min (Exp. H) and sampled for LC-MS analysis as indicated in Table 2. Also, in the case of these additional experiments, temperature, H_2O_2, dissolved O_2, and pH were measured before and after experiments.

Results of LC-MS analysis for Exp. H (given in Suppl. 4) showed that H_2O_2 (25 mg/L formed during Exp. G, which is more than the amount formed during Exps. A–F), does not affect the removal of selected micropollutants. This confirmed that the long-lived species are not the primary agents responsible for the determined removals of selected micropollutants.

Additionally, to test the hypothesis (objective iii) that the H_2O_2 formed during the combined SupCaviPlasma treatment could lead to further removal of the micropollutants in the RGHC alone, another separate experiment which is described in detail in Suppl. 5, was performed. Even though the synergistic effects of RGHC and H_2O_2 for the removal of micropollutants have already been shown in our previous studies [23], the results obtained during this study did not corroborate that. One of the possible reasons might be in lower concentration of H_2O_2 in this study (detailed discussion given in Suppl. 5).

The degradation of organic pollutants generally follows the first-order kinetics, which can be described by the following equation (Eq. (2)):

$$\ln\left(\frac{C}{C_0}\right) = -kt \tag{2}$$

where C is the remaining concentration of micropollutant (μg/L), C_0 is the initial concentration of the micropollutant (μg/L), t is the time of treatment (min) and k is the first order rate constant (min^{-1}).

Since the removals of all micropollutants behave like an exponential decay, all the measurements can be fitted with an exponential function (Eq. (3)):

$$R = 100 - 100^{*}e^{-ln2\bullet\frac{t}{t_{1/2}}}, \tag{3}$$

where $t_{1/2}$ is the half-life time when the concentration of the micropollutants is reduced to half of the initial concentration. Here we should stress that the first order rate constant k used in Eq. (2) and half-life time are related as follows: $k = \ln 2/t_{1/2}$. The results presented at 25 °C and 53 W, given in Fig. 4, Table 4 and Suppl. 6, were repeated in two parallels.

3. Results and discussion

3.1. Measurements of plasma parameters

The optical emission spectrum of the plasma generated between the electrodes inside the stable supercavitation bubble is presented in Fig. 2. Apart from the fragments of the water molecules, no other emission lines can be seen in the spectrum. The emitted light thus clearly shows only water vapor plasma. Once the stable gas bubble is formed, an oscillating electric field is applied between the electrodes. Electrons are accelerated in the electric field. The collision of fast electrons with atoms or molecules causes their excitation, dissociation, or ionization. In the gaseous plasma, water molecules are dissociated into OH molecules, O atoms, and H atoms, which is why only hydrogen atom lines (lines denoted with magenta marks), the oxygen atom lines (lines denoted with green marks), and the OH system of the emission lines (emission bands denoted with blue marks) are visible. An atom can have a lot of excited states and molecules can have even more, which is why there are more than one emission line for one specific atom and a bundle of lines, which are visible as a so-called emission band, for a particular molecule. The most prominent spectral features, in the range from 250 nm to 1,000 nm, are the hydrogen Balmer alpha and beta lines at 656 nm and 486 nm, respectively, and the OH emission system with a peak at 309 nm. There are a lot of oxygen atom emission lines, but they are not as intense as H and OH.

The optical emission spectroscopy measurements show that in the stable supercavitation bubble, there are two reactive particles with one of the highest oxidation potentials. The oxidation potentials of the $^{\bullet}OH$ molecule and O atom are 2.8 and 2.42 V (25 °C), respectively. Furthermore, as can be seen from $k_{OH}^{\bullet}$ determined for investigated micropollutants (Suppl. 1), they all have high-rate constants ranging from 8.1×10^{-11} to 1.16×10^{-10} $cm^3 \cdot molecule^{-1} \cdot s^{-1}$, indicating high susceptibility to oxidation with $^{\bullet}OH$. (Suppl. 1). Besides UV radiation (some of it is visible in Fig. 1 (B) as glowing gaseous plasma), such plasmas emit light also in the VUV (vacuum ultraviolet) region down to 100 nm. It has been shown that in plasmas, where the hydrogen 656 nm emission line is the most prominent in the visible region, most of the radiation is emitted as VUV radiation [49]. Photons in the VUV region have enough energy (up to about 10 eV) to break even the strongest bonds inside molecules. The direct impact of VUV photons on micropollutants, i.e. photolysis, can occur simultaneously with the formation of radical species and could be a possible mechanism responsible for their degradation. Only a few authors that investigated the degradation of pharmaceuticals or EDCs performed plasma diagnostics in the form of optical emission spectrum and FTIR [30,31]. The general conclusion of these studies is that whenever water is present, hydrogen radicals, oxygen radicals, and $^{\bullet}OH$ emission lines are visible due to the dissociation of water coming from the treated liquid or process gas humidity.

3.2. Removal of selected micropollutants

3.2.1. Influence of sample temperature

In these experiments, the influence of sample temperature on the removal of the investigated micropollutants during a 30-minute combined plasma-cavitation treatment in the SupCaviPlasma device was investigated. Fig. 3 shows the susceptibility of all 10 micropollutants to removal with the novel device. The highest susceptibility and thus

Table 2
Additional experiments performed to investigate the effect of SupCaviPlasma-generated H_2O_2 on the removal of selected micropollutants.

Exp.	P (W)	T (°C)	Treatment	Micropollutants	Treatment time (min)	Q (L/min)	H_2O_2 (mg/L)	O_2 (mg/L)	pH
G	24	25	Plasma + RGHC	none	45	4.9	25*	6.5*	6.7*
H	NA		Magnetic stirrer	added	0, 5, 10, 20, 30	NA	25*	7.3*	6.7*

*: measured after 30 or 45 min of treatment; NA: not available.

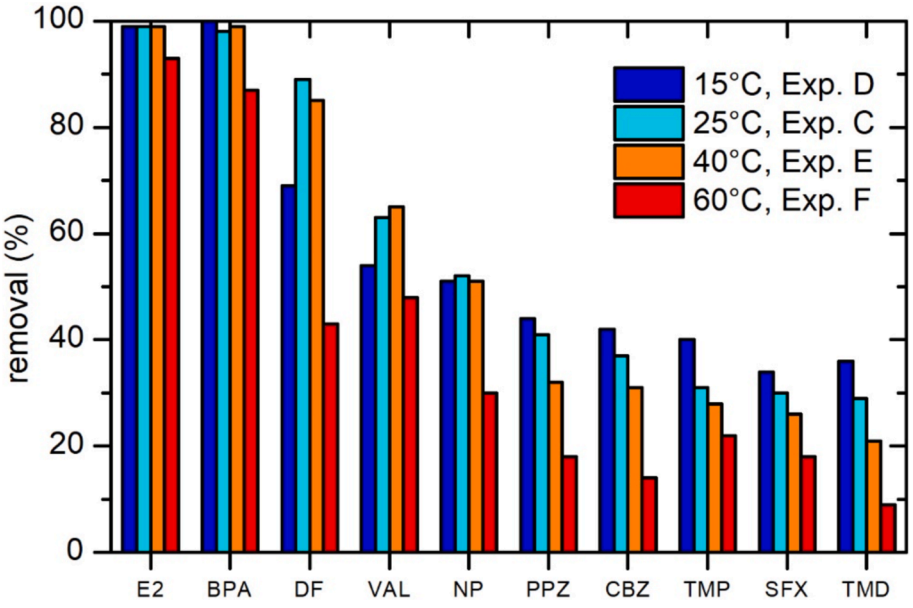

Fig. 3. Removal of investigated micropollutants (100 μg/L of each) after 30 min of SupCaviPlasma treatment at different sample temperatures. The P_{PL} during the Exps. C–F ranged from 52–61 W (Table 1).

highest removals, up to 99 %, were achieved for E2 and BPA, followed by DF, whose removal rate was up to 89 %, while the removal rates of the remaining compounds were lower. VAL and NP were removed up to 63 %, while PPZ, TMP, SFX, and TMD were removed to about 40 %. It can be seen that the removal of the compounds varied depending on the sample temperature (Fig. 3). For most micropollutants (E2, BPA, NP, PPZ, CBZ, TMP, SFX, and TMD), removal rates decreased with increasing water temperature, and the lowest removal rates of 9 to 93 % were achieved at 60 °C. This dependence can be explained by the water vapour pressure and, consequently, plasma generation and radical loss pressure dependence. As the water temperature increases, the water vapor pressure (i.e., the pressure inside the supercavitation bubble) also increases; in our case, we used water at 15, 25, 40, and 60 °C, which corresponds to water vapor pressures of 17, 32, 74, and 200 mbar, respectively. As mentioned in the introduction, the radicals generated in gaseous plasma can be lost due to three-body collisions, and the loss is proportional to the square of the pressure [50], so the density of radicals reaching the micropollutants decreases when the pressure, i.e. the water temperature, is increased. Another reason could be partially due to the lower flow rate at 60 °C compared to Exp. C–E (Table 1), which means that in Exp. F the sample went through the SupCaviPlasma 6 times less. The best results at lower temperatures (15 and 25 °C) are in perfect agreement with the requirements of (waste)water treatment, where the average annual water temperature is between these values (depending on the geographical region but typical for the EU) [50], so a treatment process that can be used at these temperatures is essential. Even though the concentration of dissolved O_2 constantly decreased during our experiments (Suppl. 3), either due to the increased temperature or due to

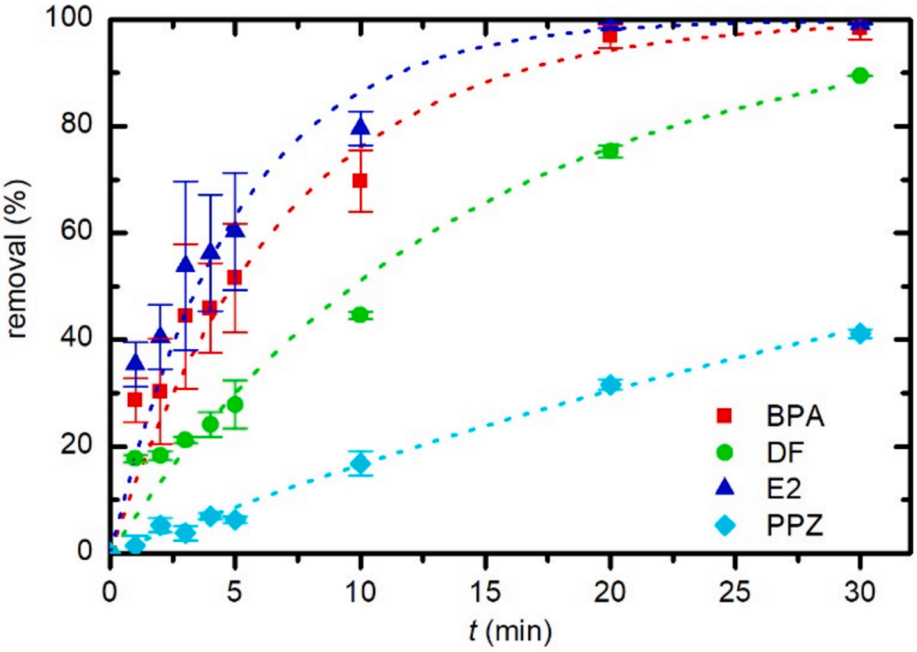

Fig. 4. Comparison of time evolutions and decay fits of BPA, DF, E2, and PPZ with SupCaviPlasma device (Exp. C: 25 °C, 53 W).

mixing in the RGHC, this had no effect on the oxidation of the micropollutants studied. Low dependence on dissolved oxygen, as shown for SupCaviPlasma, can be considered beneficial since anaerobic conditions might be encountered in WWT environment [51]. Most of the studies cited in this manuscript were conducted at room temperature, and the highest removals of the environmentally most critical compounds (E2, BPA, and DF) were achieved in Exp. C. This experiment was performed in three parallels (Figs. 4 and 5 and Suppl. 6) and obtained average values were used in all further discussions if not mentioned otherwise.

3.2.2. *Influence of physicochemical properties*

The different extent of removals of the micropollutants investigated in this study (Fig. 3 and Table 4) is most likely due to their different physicochemical properties (Suppl. 1), since for all plasma types, whether atmospheric- or sub-atmospheric-pressure, the most important factor determining the degradation rate is the location of the compounds (near the gas/liquid interface or in the bulk liquid) with respect to the location of the reactive species (gas/liquid interface). If the compounds studied are predominantly distributed in the bulk phase and not near the supercavitation bubble where the plasma species are formed, the $^{\bullet}OH$ are more likely to react with each other and form H_2O_2 before oxidizing the compounds of interest. With our unique design, we wanted to further utilize the formed H_2O_2 (see Suppl. 3) by degrading it back to $^{\bullet}OH$ under the HC generated in the RGHC [24], which unfortunately was not possible under the current experimental conditions (see Suppl. 5). As investigated micropollutants are non-volatile compounds with limited preference for partitioning into air, due to their low Henry's coefficient (Suppl. 1), this property does not play a role in the removals. The more important one is the logK_{ow}, which indicates their hydrophobicity, as compounds with higher logK_{ow} values are more likely to reach the gas/liquid interface, which increases the probability of their reaction with $^{\bullet}OH$ compared to more hydrophilic compounds (lower logK_{ow} values) predominately distributed in the bulk liquid [3,22,40,52]. The logK_{ow} values for the investigated compounds range from 0.48 to 4.51 (Suppl. 1), where the compounds removed to the highest extent (E2, BPA, and DF) all have logK_{ow} values higher than 3.51, which makes it more likely that they were located on the gas/liquid interface (in more detail discussed in Section 3.2.3). One of the reasons why VAL (also with a high logK_{ow} value) was removed to a lower extent, could be its peculiar chemical structure. As the VAL molecule includes both −NH and −COOH functional groups, its solubility is heavily governed by the *pH* [53], which decreased during all our experiments (see Suppl. 3) and by changing its solubility its removal was enhanced. This can also be deducted from its time evolution graph given in Suppl. 6, where a lower removal rate i.e. higher $t_{1/2}$ compared to DF was determined, despite a similar logK_{ow} value. Furthermore, even though also DF has both, acidic and basic functional groups in its structure (Suppl. 1), this does not affect its solubility. Firstly, because DF has $COO^{-}Na^{+}$ and secondly because the −NH group in DF is not basic but acidic, due to the presence of two −Cl atoms in ortho positions, which are electronegative functional groups. These results show that many hydrophobic compounds can be simultaneously removed with SupCaviPlasma.

Another important physicochemical property that influences the removal of micropollutants is the *pKa* value, which describes the degree of ionization of a compound at a known *pH* value. Ionized and non-ionized molecules have different properties, with ionized molecules generally having higher water solubility and are expected to be present in the aquatic environment, while non-ionized molecules have more hydrophobic properties and are more likely to be at the interface between the supercavitation bubble and the liquid [54]. This property

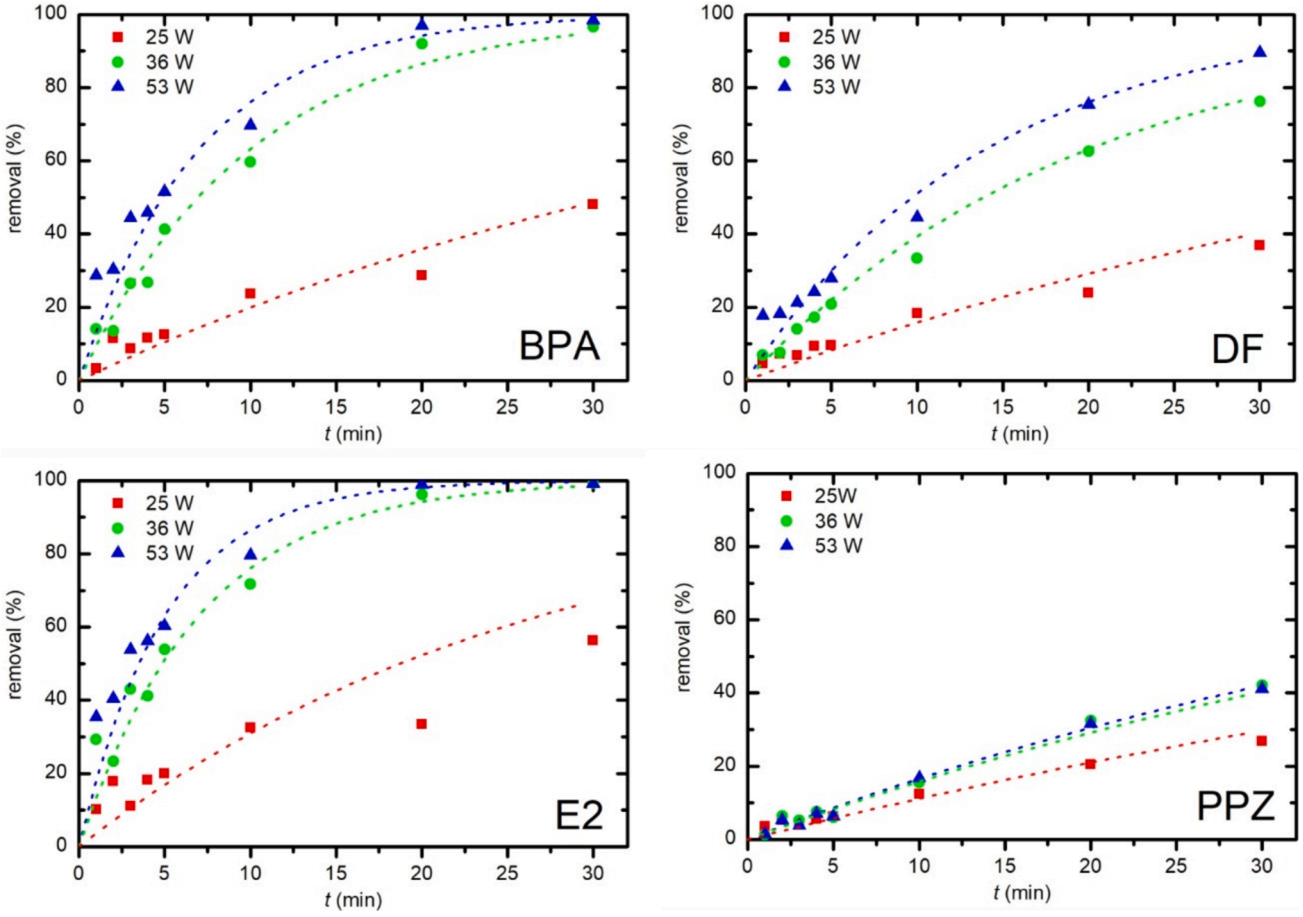

Fig. 5. Removals of BPA, DF, E2, and PPZ during plasma-cavitation treatment (25 °C) at different plasma powers.

could be an explanation for the lower removal rates of NP despite its high logK_{OW} value of 3.1 (see Suppl. 1). Its *pKa* value is 4.15 (Suppl. 1), which means that at *pH* above this value, the −COOH group of NP is in ionized form, making it more soluble and therefore more likely to be present in the bulk liquid. From the results presented in Suppl. 3, it can be seen that the *pH* value decreased throughout our experiments, from initial values between 6.7 and 8.7 down to values between 4.3 and 5.9, depending on the experiment. The reason for the different values determined in the initial samples could be due to different amounts of dissolved CO_2, as discussed by Banschik et al. [2]. The drop in *pH* in atmospheric-pressure plasmas is usually attributed to the formation of various nitrogen species, such as acids and nitrates [2,3,31]. Since these species are not formed in the SupCaviPlasma device, the reason for the drop in *pH* is most likely due to the partial degradation of the investigated compounds to organic acids, as discussed in [5,35], or to the formation of the secondary oxidant, H_2O_2 [7]. Another possible cause could be the formation of formic acid from methanol, which was used as a solvent for the preparation of the standard solutions of the micropollutants. When plasmas are considered for industrial applications, the *pH* drop does not play a major role as the WW components act as a buffer system and mitigate this effect. However, when the technology is considered for less complex matrices such as surface or drinking water, a more conservative *pH* drop is an attribute, and here SupCaviPlasma has an advantage over atmospheric-pressure plasmas, where the *pH* can drop down to 2–3.5 [5,29,31].

3.2.3. Time evolution of removal

As the highest removal was achieved at 25 °C for most micropollutants, this temperature was chosen for further investigation of the time evolution of micropollutant removal (Fig. 3: Exp. C). A detailed time-lapse comparison of the removal of four selected compounds that were either removed to the highest extent (Fig. 3: BPA, DF, and E2) or investigated for the first time in the plasma-cavitation treatment (PPZ) is shown in Fig. 4. The time evolutions, their exponential decay fits, and the half-life times of the compounds removed to a lesser extent – VAL, SFX, CBZ, TMP, TMD, and NP – are shown in Suppl. 6.

Fig. 4 shows that the removal rates of BPA, DF, E2, and PPZ are different. The reason for this is most likely due to their physico-chemical properties and their different chemical structure (Suppl. 1) as mentioned in Section 3.2.2.

The first requirement for the effectiveness of AOPs such as plasma or HC for the degradation of organic compounds is that they are located where the •OH are formed (at the gas–liquid interface), which is governed by their n-octanol/water partition coefficient (logK_{OW}) (see Section 3.2.2). Since E2, BPA, and DF all have a log$K_{OW} \geq 3.32$ (Suppl. 1), this condition is met. The next important requirement is that they must be susceptible to oxidation with formed reactive species, in our case •OH, which strongly depends on their chemical structure. QSAR studies have shown that the presence of activated aromatics in organic compounds containing functional groups such as $-NH_2$, −NH, and −OH, which can activate the benzene molecule, increase their susceptibility to react with •OH [55,56]. The presence of −OH, which is an electron donor, directs the •OH to ortho and para positions [57]. This may be the mechanism responsible for the rapid and comparable removal of E2 and BPA, both of which have aromatic −OH groups in their structure. For DF, which has a very weak electron donor −NH group due to two electronegative chlorine atoms in its structure, a slightly slower degradation was observed (see Suppl. 1). One of the possible reasons why DF was still so effectively removed was also the notable decrease in *pH* during the experiment (Suppl. 3), which fell to a value close to the *pKa* of DF, which, as was previously shown, increases the susceptibility of DF to oxidation [58]. The lower the DF ionization at decreasing *pH*, the higher is presumably also its distribution at the gas–liquid interface, where the reactive species are formed, and consequently, the higher is its degradation rate. The main reason for the very slow and low degradation of PPZ could be primarily due to its low logK_{OW} value of 2.05, while the presence of methyl and propyl groups in its pyrazole ring, which could sterically hinder the reaction of PPZ with •OH, plays a less important role.

Higher hydrophilicity (lower logK_{ow} value) and/or the presence of electron acceptor groups together with the absence of electron donor groups on aromatic rings could be the main reasons for the comparatively slower removal of the other compounds tested (CBZ, TMP, SFX, and NP). Removals of VAL and TMD are discussed in Sections 3.2.2 and 3.3.1 in more detail.

3.2.4. Influence of plasma power

In these experiments, the influence of different plasma powers on the removal rate of the investigated micropollutants was investigated. Fig. 5. shows the exponential dependence of the removal of BPA, DF, E2, and PPZ during a 30-minute treatment at 25 °C (selected based on the results shown in Fig. 3) and three different plasma powers: 25, 36, and 53 W. Fig. 5 shows that the removal of micropollutants increases with increasing plasma power for all four compounds. In the case of E2 and BPA, removals of 97 % were achieved at 36 and 53 W, whereas in the case of DF, removals of 76 and 89 % were achieved. At the lowest plasma power (25 W), a significantly lower removal of all three micropollutants of 37 to 56 % was achieved. In the case of PPZ, the differences in removal between the different plasma powers were not as pronounced. The removals of VAL, TMP, CBZ, TMD, SFX, and NP followed similar trends, with the highest removals obtained at the highest applied plasma power. The removals at 25 and 36 W were between 32–51 % and 28–65 %, respectively (Suppl. 7).

Half-life removal times for BPA, DF, E2, and PPZ with plasma-cavitation treatment at different plasma powers are presented in Table 3. Evidently, the removal rate does not follow the linear power increase. When the power was doubled, the removal rate increased more than six times for BPA, four times for DF, five times for E2, and approximately 1.5 times for PPZ.

The effect of plasma power has also been investigated in other studies. Gao et al. [11] showed that by increasing the peak voltage of the DBD from 10 to 13 kV, the removal of E2 increased from about 66 % to 100 % within 30 min. Similarly, Guo et al. [35] showed an increase in BPA removal from 66 to 95 % when they increased the discharge voltage in the PSD from 16 to 20 kV, while Yang et al. [36] demonstrated an 80 % increase in BPA removal when the discharge voltage was increased from 6.8 to 16.8 kV (plasma power was 412.5 W). This was attributed to the increase in the electric discharge field, shock waves, and UV irradiation, which increased the amount of reactive species in both the gas and liquid phases [7,11,36]. Similar to our case, Wardenier et al. [7] also concluded that the increase in power does not affect all studied micropollutants to the same extent and therefore depends on the compound, as shown in our study. It should also be emphasized that in our case, 10 compounds were treated simultaneously, which means that after the first few minutes, in addition to the original compounds, their degradation products also competed for the reactive species, which could affect the removal rate of the original micropollutants (see Section 3.3.1). The correlation between the removal rate and the increase in plasma power would be similar for all micropollutants if only one micropollutant was present in treated water at a time. In this case, the increase in removal rate due to the increase in plasma power would

Table 3
Half-life times ($t_{1/2}$) for different micropollutants when treating them with plasma-cavitation with different plasma powers at 25 °C sample temperature.

Micropollutant	25 W $t_{1/2}$ [min]	36 W $t_{1/2}$ [min]	53 W $t_{1/2}$ [min]
BPA	31	7	5
DF	40	14	10
E2	19	5	3.5
PPZ	59	40	38

likely be similar for all micropollutants. Liu et al. [6], on the other hand, showed an increase in DF removal when only the discharge voltage was increased from 4 to 6 kV and a decrease at 8 kV. They attributed this to charge accumulation and discharge instability, which leads to a decreased formation of reactive species.

3.3. SupCaviPlasma in comparison to atmospheric-pressure plasmas

3.3.1. Comparison of removals

The literature search revealed that different types of plasma have been investigated for the removal of the micropollutants studied and that the removal rates achieved vary (Table 4). It must be acknowledged that a direct comparison of the removal rates obtained in SupCaviPlasma with other plasma types is not optimal since in atmospheric-pressure plasmas, O_3 is formed in addition to $^{\bullet}OH$, which readily oxidizes some compounds [38], but nevertheless, some general observations can still be made. As in our study, E2 and BPA were removed more than 95 % in other plasma setups regardless of the initial concentration (Table 4). Gao et al. [11] achieved complete removal of E2 with DBD in 30 min at the same initial concentration as in this study, while in two studies by Guo et al. [35] and Yang et al. [36], they removed much higher initial concentrations of BPA with PSD and DBD plasmas, respectively. A possible reason is that in our study, 10 structurally different compounds with high k_{OH} values (see Suppl. 1), all competing for $^{\bullet}OH$, were investigated simultaneously. In addition, degradation products formed after the reaction of the original compounds with $^{\bullet}OH$ also compete for the generated reactive species influencing the removal of the original compounds, as discussed by Gao et al. [11] and Zupanc et al. [54]. In contrast to these results, Wardenier et al. [7] achieved only about 48 % of BPA removal in DBD in 30 min, which they attributed to lower production rates of reactive species (O_3 and $^{\bullet}OH$) when air was used as the feed gas. Comparable to our results, high removal of DF was achieved with PCD and plasma microbubble treatment ($\geq$ 91 %) [3,6,28,29], while only up to 50 % removal was demonstrated for DBD plasma generated in air [38]. The authors attributed the low removal to the formation of fewer reactive species in the air compared to other gases such as Ar or O_2. Not many studies are available for VAL, but Raji et al. [30] showed the removal of only 24 % in 10 min using a JET plasma, which could only be increased by adding a catalyst. On the other hand, under optimal experimental conditions, higher removals than in our study were obtained for NP, TMP, TMD, SFX, and CBZ (Table 4). However, in the case of NP [37] and TMD [4], at similar solution *pH,* the removals are comparable to our study. For TMD, removal was shown to be greatly increased and much faster in alkaline media compared to neutral and acidic media (as in our study, see Suppl. 3). The authors attributed this to the deprotonation of TMD in alkaline media, which enhanced its nucleophilic and hydrophobic properties, making it more prone to react with $^{\bullet}OH$ and near the site where these reactive species are formed [3,4]. With TPM, an optimal removal (66 min) of up to 85 % was achieved, while the removal at 33 min was lower, up to 65 % [2]. The same applies to SFX and CBZ when treated with DBD plasma in air, whose removal after 30 min treatment time was about 30 and 50 % lower, respectively, compared to the 90 min specified in Table 4 [32,39]. Although a direct comparison of effectiveness between different plasma types is difficult due to the different numbers and concentrations of compounds treated simultaneously, sample volumes, and treatment times, SupCaviPlasma removed 10 compounds exclusively by the formed $^{\bullet}OH$ (when comparing the effect of reactive plasma species), with removals ranging from 29–99 %. If alternative treatments have any chance at all of being considered for scale-up, studies investigating the removal of a mixture of compounds are extremely important as they are closer to the real-life scenario. In addition, compounds recalcitrant to biological treatment have been shown to have serious environmental effects, namely E2, BPA, and DF, and have been removed to the highest extent (with $t_{1/2}$ 10 min or less). These removals also satisfy the $\geq$ 80 % removal rates being considered inside the EU legislation. Furthermore, the identification and possible toxicity of the formed oxidation products would have to be determined in future experiments [59].

Table 4
Comparison of the effectiveness and efficiency of different plasma setups with SupCaviPlasma under optimal experimental conditions.

Compound	Plasma	P_{PL}/P_{RGHC} (W)	V (L)	C_0(mg/L)	Time(min)	Removal(%)	$t_{1/2}$ (min)	$G_{PL}/G_{PL+RGHC}$ (mg/kWh)	Ref.
VAL	JET	NA	NA	44	10	24	76 [a]	NA	[30]
	SupCaviPlasma	53/530	3	0.1	30	63 ± 2	21	G_{90} = 4 / 0.4	This study
TMP	PCD	28.28	0.3	0.5	66	85	24 [a]	G_{90} = 11	[2]
	SupCaviPlasma	53/530	3	0.1	30	31 ± 6	52	G_{90} = 2 / 0.2	This study
PPZ	**SupCaviPlasma**	53/530	3	0.1	30	41 ± 1	38	G_{90} = 2 / 0.2	This study
TMD	PCD	9	10	8.8	28	90	8 [a]	20,000[b]	[4]
	SupCaviPlasma	53/530	3	0.1	30	29 ± 4	62	G_{90} = 1 /0.1	This study
E2	DBD	765[b]	0.5	0.1	30	100	5.3	G_{90} = 0.22	[11]
	SupCaviPlasma	53/530	3	0.1	30	99 ± 1	3.5	G_{90} = 26 /2.4	This study
BPA	PSD	NA/NA	NA	20	60	95.3	5 [a]	NA	[35]
	DBD	412	0.5	50	30	100	5 [a]	G_{100} = 145[c]	[36]
	SupCaviPlasma	53/530	3	0.1	30	98 ± 2	5	G_{100} = 11 / 1	This study
NP	DBD	60	NA	20	6	93.2	2 [a]	NA	[37]
	SupCaviPlasma	53/530	3	0.1	30	52 ± 6	28	G_{90} = 3 / 0.3	This study
SFX	DBD	NA	NA	50	90	94	22 [a]	G_{60} = 1,720	[39]
	SupCaviPlasma	53/530	3	0.1	30	30 ± 3	55	G_{60} = 2.8 / 0.3 G_{90} = 2 / 0.2	This study
CBZ	PCD	59	0.001	0.2	24	>99	2 [a]	G_{90} = 26	[28]
	DBD	500	1	24	90	99	14 [a]	G_{90} = 85[c]	[32]
	SupCaviPlasma	53/530	3	0.1	30	37 ± 4	42	G_{90} = 2 / 0.2	This study
DF	PCD	9	10	10	11	100	ND	G_{90} = 50,000	[3]
	JET	200	0.25	25	30	100	5	G_{100} = 1,500	[29]
	DBD	150	0.5	50	30	50	30 [a]	G_{50} = 1,500	[38]
	SupCaviPlasma	53/530	3	0.1	30	89 ± 1	10	G_{50} = 17 / 1.5 G_{90} = 9 / 0.8 G_{100} = 5 / 0.5	This study

C_0: initial concentration of the compounds; [a]: $t_{1/2}$ was assessed based on available data; [b]: % for calculation of G not specified; [c]: calculated by the authors; NA: not available; $G_{60/90/100}$: calculated if 60/90/100 % of the micropollutant was degraded; P_{PL}: power for plasma generation; P_{RGHC}: power for rotational generator of hydrodynamic cavitation; ND: cannot be determined.

3.3.2. Comparison of reactive species formed

Regardless of the micropollutants studied or the type of plasma used, most studies point to oxidation by •OH formed from water molecules or from the decomposition of O_3 as the primary degradation mechanism [2,6,30,36,37], followed by direct O_3 oxidation [11,38] and even nitrification by N species [8,31]. Since the formation of H_2O_2 is commonly used as an indicator for the formation of •OH in plasmas [2], its concentration is frequently measured and ranges from 30−70 mg/L after 30 min treatment times [2,26,28,36]. Its formation confirms the transport of •OH formed in the gas phase into the liquid phase [7,31]. In addition to the results shown in Fig. 2, the H_2O_2 concentrations between 15 and 18.5 mg/L determined after each SupCaviPlasma treatment (see Suppl. 3) also confirm the transport of •OH from the supercavitation bubble into the liquid phase in our setup. On this basis, the determined removals in our study are also most likely due to the oxidation of micropollutants with •OH, which is consistent with other studies investigating different plasma types [2,5,28,30,38]. It should be pointed out that in our case, •OH are likely formed to the highest extent inside the supercavitation bubble due to plasma discharge, while the possibility of their formation inside the RGHC due to developed cavitation or even at the supercavitation closure (marked at Fig. 1 (A)) where the stable bubble breaks down into the flow regime with imploding cavities, also exists. While the possibility of these effects does not deteriorate the outcome and the novelty of the present study, it calls for further exploration in the future.

That •OH generated are mainly responsible for the removal, was additionally corroborated by Exp. H, which confirms that H_2O_2 plays no role in the degradation of the original compounds (Suppl. 4). Since the formation of by-products is unfavourable in water treatment technologies as they need to be removed before the treated water is released or re-used, which increases costs, SupCaviPlasma shows potential as the amount of H_2O_2 formed after 30 min was lower compared to other plasma devices. Furthermore, compared to atmospheric-pressure plasmas, in which H_2O_2 and O_3 are formed, in SupCaviPlasma, only the former is formed as a by-product.

3.3.3. Comparison of efficiency

Table 4 shows that the $t_{1/2}$ of selected micropollutants was between 3.5 and 62 min under optimized test conditions. The lowest half-lives were achieved for the compounds removed to the highest extent. As already mentioned, it is very difficult to directly compare the half-lives determined in different studies, as they were carried out under different experimental conditions and mostly for individual substances. To make the comparisons more precise, the authors performed some calculations based on the data available in these studies (see legend in Table 4). According to these calculations, better performance or similar degradation half-lives of VAL, E2, BPA, and DF, were achieved in the SupCaviPlasma compared to other plasma devices. On the other hand, better $t_{1/2}$ of TMP, TMD, NP, SFX, and CBZ were determined in atmospheric-pressure plasma devices. Similarly, energy yields can also be correlated to the removals and the highest G_{PL90}-values between 9 and 26 mg/kWh (Table 4) were obtained for E2, BPA, and DF. If we also consider the $P_{PL+RGHC}$, the calculated G_{90} values drop by a factor of about ten (from 0.8 to 2.4 mg/kWh). With RGHC optimization or even its replacement with a pump [45], even higher removals could be obtained. We can see (Table 4) that the *G*-values determined for the selected micropollutants with different plasma devices vary greatly and that the atmospheric-pressure plasma devices at first glance outperform SupCaviPlasma for most micropollutants except E2. However, the direct comparison of *G*-values could be misleading as they were obtained at different C_0 values and under different experimental conditions (i.e. single or multiple compounds). Furthermore, while calculating *G*-values, as we see in Eq. (1), one can achieve the same numerator C_0V with either a large volume and low initial concentration or with a small volume and high initial concentration of micropollutant. It is obvious that higher *G*-values can be obtained while using higher C_0 values and lower volumes of water. The comparison of G-values is therefore only useful when similar volumes of treated water and initial concentrations of micropollutants are used. It is important to note that with the SupCaviPlasma, the highest *G*-values were obtained for the most environmentally critical micropollutants (BPA, E2, and DF) at higher concentrations than those found in the environment. It should also be noted that in many studies the sum of all energy requirements is often missing, and the reported *G*-values should therefore only be used for guidance and the same holds true for EEO-values (Suppl. 8). It is to be expected that the efficiency of the process decreases, and the *G*-values increase when the technology is applied to more complex matrices such as WW. An advantageous aspect of this novel design is that it is a flow-through system and that the RGHC part of SupCaviPlasma already acts as a pump, so no additional device is needed for scale-up.

4. Conclusion

In the present study, the simultaneous removal of 10 emerging contaminants (valsartan, trimethoprim, sulfamethoxazole, naproxen, diclofenac, tramadol, propyphenazone, carbamazepine, 17β-estradiol and bisphenol A) at a concentration of 100 μg/L was evaluated using a novel device combining sub-atmospheric-pressure plasma and hydrodynamic cavitation (SupCaviPlasma). The main conclusions of the study are as follows:

- Removal effectiveness and efficiency depend on sample temperature, treatment time, physico-chemical properties, chemical structure and plasma power.
- The highest removals of all compounds were achieved at 25 °C, 30 min and 53 W plasma power.
- The most important compound properties influencing their removals were logK_{OW} and *pKa*.
- The compounds with high logK_{OW} values (17β-estradiol, bisphenol A, and diclofenac) were removed to the highest extent, namely ≥ 89 %.
- The removal of the other compounds was between 33 and 65 %.
- The estimation of the energy required for the removal of micropollutants was calculated as G_{90} and ranged between 1 and 26 mg/kWh.
- The advantage of SupCaviPlasma is that the plasma is generated only in water vapour, resulting in the formation of mainly •OH, fewer by-products (e.g. nitrates, O_3, and H_2O_2) and lesser *pH* drop.

Despite the very encouraging results in the case of two endocrine-disrupting compounds, 17β-estradiol and bisphenol A, whose potent endocrine effects occur at ng/L concentrations, and diclofenac, whose recalcitrance to biological treatment has been repeatedly demonstrated, it must be recognized that this study was conducted only as a proof-of-concept. To fully evaluate the potential of SubCaviPlasma, further studies are required, first examining the degree of mineralization, followed by toxicological studies confirming the environmental safety of such a process, and finally, studies conducted in more complex matrices. Nonetheless, the results of this study shed light on what can be achieved by using a sub-atmospheric-pressure plasma in conjunction with hydrodynamic cavitation and will serve as a starting point for future device optimizations. The findings from studies like this could contribute to the development of novel and sustainable water treatment technologies. which would ultimately facilitate the protection and conservation of our precious water resources in the face of increasing pollution.

CRediT authorship contribution statement

Mojca Zupanc: Writing – review & editing, Writing – original draft, Investigation, Funding acquisition. **Gregor Primc:** Writing – review & editing, Writing – original draft, Visualization, Formal analysis, Data curation. **Matevž Dular:** Writing – review & editing, Resources, Funding

acquisition. **Martin Petkovšek:** Writing – review & editing, Visualization, Investigation, Formal analysis. **Robert Roškar:** Writing – review & editing, Resources, Funding acquisition. **Rok Zaplotnik:** Writing – review & editing, Visualization, Formal analysis, Data curation. **Jurij Trontelj:** Writing – review & editing, Writing – original draft, Resources, Funding acquisition, Formal analysis.

Declaration of competing interest

The authors declare that they have no known competing financial interests or personal relationships that could have appeared to influence the work reported in this paper.

Acknowledgements

The authors acknowledge the financial support from the Slovenian Research Agency (research project No. J2-4480, J2-3044, L7-3184, research core funding No. P2-0401, P2-0422, P2-0082, P1-0189).

Appendix A. Supplementary data

Supplementary data to this article can be found online at https://doi.org/10.1016/j.ultsonch.2024.107110.

References

[1] R. Hernández-Tenorio, E. González-Juárez, J.L. Guzmán-Mar, L. Hinojosa-Reyes, A. Hernández-Ramírez, Review of occurrence of pharmaceuticals worldwide for estimating concentration ranges in aquatic environments at the end of the last decade, Journal of Hazardous Materials Advances 8 (2022) 100172, https://doi.org/10.1016/j.hazadv.2022.100172.

[2] R. Banaschik, P. Lukes, H. Jablonowski, M.U. Hammer, K.D. Weltmann, J.F. Kolb, Potential of pulsed corona discharges generated in water for the degradation of persistent pharmaceutical residues, Water Res 84 (2015) 127–135, https://doi.org/10.1016/j.watres.2015.07.018.

[3] V. Derevshchikov, N. Dulova, S. Preis, Oxidation of ubiquitous aqueous pharmaceuticals with pulsed corona discharge, J Electrostat 110 (2021), https://doi.org/10.1016/j.elstat.2021.103567.

[4] D. Nikitin, B. Kaur, S. Preis, N. Dulova, Persulfate contribution to photolytic and pulsed corona discharge oxidation of metformin and tramadol in water, Process Saf. Environ. Prot. 165 (2022) 22–30, https://doi.org/10.1016/j.psep.2022.07.002.

[5] K.S. Kim, S.K. Kam, Y.S. Mok, Elucidation of the degradation pathways of sulfonamide antibiotics in a dielectric barrier discharge plasma system, Chem. Eng. J. 271 (2015) 31–42, https://doi.org/10.1016/j.cej.2015.02.073.

[6] Q. Liu, W. Ouyang, X. Yang, Y. He, Z. Wu, K. (Ken) Ostrikov, Plasma-microbubble treatment and sustainable agriculture application of diclofenac-contaminated wastewater, Chemosphere 334 (2023). https://doi.org/10.1016/j.chemosphere.2023.138998.

[7] N. Wardenier, P. Vanraes, A. Nikiforov, S.W.H. Van Hulle, C. Leys, Removal of micropollutants from water in a continuous-flow electrical discharge reactor, J Hazard Mater 362 (2019) 238–245, https://doi.org/10.1016/j.jhazmat.2018.08.095.

[8] B. Topolovec, N. Škoro, N. Puač, M. Petrovic, Pathways of organic micropollutants degradation in atmospheric pressure plasma processing – A review, Chemosphere 294 (2022), https://doi.org/10.1016/j.chemosphere.2022.133606.

[9] L.H.M.L.M. Santos, A.N. Araújo, A. Fachini, A. Pena, C. Delerue-Matos, M.C.B.S. M. Montenegro, Ecotoxicological aspects related to the presence of pharmaceuticals in the aquatic environment, J Hazard Mater 175 (2010) 45–95, https://doi.org/10.1016/j.jhazmat.2009.10.100.

[10] S.N. Nam, C.E. Choong, S. Hoque, T.I. Farouk, J. Cho, M. Jang, S.A. Snyder, M. E. Meadows, Y. Yoon, Catalytic non-thermal plasma treatment of endocrine disrupting compounds, pharmaceuticals, and personal care products in aqueous solution: A review, Chemosphere 290 (2022), https://doi.org/10.1016/j.chemosphere.2021.133395.

[11] L. Gao, L. Sun, S. Wan, Z. Yu, M. Li, Degradation kinetics and mechanism of emerging contaminants in water by dielectric barrier discharge non-thermal plasma: The case of 17β-Estradiol, Chem. Eng. J. 228 (2013) 790–798, https://doi.org/10.1016/j.cej.2013.05.079.

[12] J.E. Foster, Plasma-based water purification: Challenges and prospects for the future, Phys Plasmas 24 (2017), https://doi.org/10.1063/1.4977921.

[13] V. Kumar, S.K. Lakkaboyana, N. Sharma, P. Chakraborty, M. Umesh, R. Pasrija, J. Thomas, V.U. Kalebar, I. Jayaraj, M.K. Awasthi, T. Das, A.A. Oladipo, D. Barcelo, L.F. Dumee, A critical assessment of technical advances in pharmaceutical removal from wastewater – A critical review, Case Studies in Chemical and Environmental Engineering 8 (2023), https://doi.org/10.1016/j.cscee.2023.100363.

[14] European Commission, Water Framework Directive, (2000). https://environment.ec.europa.eu/topics/water/water-framework-directive_en (accessed November 21, 2023).

[15] European Commission, EU Zero pollution legislative package, (n.d.). https://ec.europa.eu/search/index.do?QueryText=the+zero+pollution+package&op=Search&swlang=en (accessed November 21, 2023).

[16] M. Gągol, A. Przyjazny, G. Boczkaj, Wastewater treatment by means of advanced oxidation processes based on cavitation – A review, Chem. Eng. J. 338 (2018) 599–627, https://doi.org/10.1016/j.cej.2018.01.049.

[17] D. Kanakaraju, B.D. Glass, M. Oelgemöller, Advanced oxidation process-mediated removal of pharmaceuticals from water: A review, J Environ Manage 219 (2018) 189–207, https://doi.org/10.1016/j.jenvman.2018.04.103.

[18] J. Iqbal, N.S. Shah, J. Ali Khan, M. Naushad, G. Boczkaj, F. Jamil, S. Khan, L. Li, B. Murtaza, C. Han, Pharmaceuticals wastewater treatment via different advanced oxidation processes: Reaction mechanism, operational factors, toxicities, and cost evaluation – A review, Sep Purif Technol 347 (2024). https://doi.org/10.1016/j.seppur.2024.127458.

[19] Y. Benito, S. Arrojo, G. Hauke, P. Vidal, Hydrodynamic Cavitation As A Low-cost AOPFor Wastewater Treatment: Preliminary ResultsAnd A New Design Approach, WIT Trans. Ecol. Environ. 80 (2005), https://doi.org/10.2495/WRM050501.

[20] M. Dular, T. Griessler-Bulc, I. Gutierrez-Aguirre, E. Heath, T. Kosjek, A. Krivograd Klemenčič, M. Oder, M. Petkovšek, N. Rački, M. Ravnikar, A. Šarc, B. Širok, M. Zupanc, M. Žitnik, B. Kompare, Use of hydrodynamic cavitation in (waste)water treatment, Ultrason Sonochem 29 (2016), https://doi.org/10.1016/j.ultsonch.2015.10.010.

[21] M. Zupanc, Ž. Pandur, T. Stepišnik Perdih, D. Stopar, M. Petkovšek, M. Dular, Effects of cavitation on different microorganisms: The current understanding of the mechanisms taking place behind the phenomenon. A review and proposals for further research, Ultrason Sonochem 57 (2019) 147–165, https://doi.org/10.1016/j.ultsonch.2019.05.009.

[22] M. Zupanc, T. Kosjek, M. Petkovšek, M. Dular, B. Kompare, B. Širok, Ž. Blažeka, E. Heath, Removal of pharmaceuticals from wastewater by biological processes, hydrodynamic cavitation and UV treatment, Ultrason Sonochem 20 (2013) 1104–1112, https://doi.org/10.1016/j.ultsonch.2012.12.003.

[23] E.R. Bandala, O.M. Rodriguez-Narvaez, On the Nature of Hydrodynamic Cavitation Process and Its Application for the Removal of Water Pollutants, Air, Soil and Water Research 12 (2019), https://doi.org/10.1177/1178622119880488.

[24] M. Zupanc, T. Kosjek, M. Petkovšek, M. Dular, B. Kompare, B. Širok, M. Stražar, E. Heath, Shear-induced hydrodynamic cavitation as a tool for pharmaceutical micropollutants removal from urban wastewater, Ultrason Sonochem 21 (2014), https://doi.org/10.1016/j.ultsonch.2013.10.025.

[25] J. Gostiša, M. Zupanc, M. Dular, B. Širok, M. Levstek, B. Bizjan, Investigation into cavitational intensity and COD reduction performance of the pinned disc reactor with various rotor-stator arrangements, Ultrason Sonochem 77 (2021), https://doi.org/10.1016/j.ultsonch.2021.105669.

[26] K. Fedorov, K. Dinesh, X. Sun, R. Darvishi Cheshmeh Soltani, Z. Wang, S. Sonawane, G. Boczkaj, Synergistic effects of hybrid advanced oxidation processes (AOPs) based on hydrodynamic cavitation phenomenon – A review, Chemical Engineering Journal 432 (2022). https://doi.org/10.1016/j.cej.2021.134191.

[27] J.-P. Franc, J.-M. Michel, Fundamentals of Cavitation (2005).

[28] R.K. Singh, L. Philip, S. Ramanujam, Continuous flow pulse corona discharge reactor for the tertiary treatment of drinking water: Insights on disinfection and emerging contaminants removal, Chem. Eng. J. 355 (2019) 269–278, https://doi.org/10.1016/j.cej.2018.08.109.

[29] A. Kumar, N. Škoro, W. Gernjak, O. Jovanović, A. Petrović, S. Živković, E. C. Lumbaque, M.J. Farré, N. Puač, Degradation of diclofenac and 4-chlorobenzoic acid in aqueous solution by cold atmospheric plasma source, Sci. Total Environ. 864 (2023), https://doi.org/10.1016/j.scitotenv.2022.161194.

[30] A. Raji, K.N. Pandiyaraj, D. Vasu, M.C. Ramkumar, R.R. Deshmukh, V. Kandavelu, Non-equilibrium atmospheric pressure plasma assisted degradation of the pharmaceutical drug valsartan: Influence of catalyst and degradation environment, RSC Adv 10 (2020) 35709–35717, https://doi.org/10.1039/d0ra05608a.

[31] A. Kovačič, M. Modic, N. Hojnik, M. Štampar, M.R. Gulin, C. Nannou, L. A. Koronaiou, D. Heath, J.L. Walsh, B. Žegura, D. Lambropoulou, U. Cvelbar, E. Heath, Degradation and toxicity of bisphenol A and S during cold atmospheric pressure plasma treatment, J Hazard Mater 454 (2023), https://doi.org/10.1016/j.jhazmat.2023.131478.

[32] H. Krause, B. Schweiger, E. Prinz, J. Kim, U. Steinfeld, Degradation of persistent pharmaceuticals in aqueous solutions by a positive dielectric barrier discharge treatment, J Electrostat 69 (2011) 333–338, https://doi.org/10.1016/j.elstat.2011.04.011.

[33] K. Kučerová, Z. Machala, K. Hensel, Transient Spark Discharge Generated in Various N2/O2 Gas Mixtures: Reactive Species in the Gas and Water and Their Antibacterial Effects, Plasma Chem. Plasma Process. 40 (2020) 749–773, https://doi.org/10.1007/s11090-020-10082-2.

[34] D. Gerrity, B.D. Stanford, R.A. Trenholm, S.A. Snyder, An evaluation of a pilot-scale nonthermal plasma advanced oxidation process for trace organic compound degradation, Water Res 44 (2010) 493–504, https://doi.org/10.1016/j.watres.2009.09.029.

[35] H. Guo, H. Wang, Q. Wu, J. Li, Degradation and mechanism analysis of bisphenol A in aqueous solutions by pulsed discharge plasma combined with activated carbon, Sep Purif Technol 190 (2018) 288–296, https://doi.org/10.1016/j.seppur.2017.09.002.

[36] J. Yang, D. Zeng, M. Hassan, Z. Ma, L. Dong, Y. Xie, Y. He, Efficient degradation of Bisphenol A by dielectric barrier discharge non-thermal plasma: Performance,

degradation pathways and mechanistic consideration, Chemosphere 286 (2022), https://doi.org/10.1016/j.chemosphere.2021.131627.
[37] J.Q. Wang, B.G. Zheng, J.B. Zhang, Z. Zheng, Degradation of the Emerging Contaminant Naproxen in Aqueous Solutions by Dielectric Barrier Discharge, Asian J. Chem. 25 (2013) 3595–3600. https://doi.org/10.14233/ajchem.2013.13668.
[38] K.H. Hama Aziz, H. Miessner, S. Mueller, D. Kalass, D. Moeller, I. Khorshid, M.A. M. Rashid, Degradation of pharmaceutical diclofenac and ibuprofen in aqueous solution, a direct comparison of ozonation, photocatalysis, and non-thermal plasma, Chemical Engineering Journal 313 (2017) 1033–1041, https://doi.org/10.1016/j.cej.2016.10.137.
[39] P. Manoj, K. Reddy, C. Subrahmanyam, Catalytic Plasma Reactor for Degradation and Mineralization of Pharmaceuticals and Personal Care Products, J. Adv. Oxid. Technol 18 (2015) 161.
[40] A. Kovačič, D. Škufca, M. Zupanc, J. Gostiša, B. Bizjan, N. Krištofelc, M.S. Dolenc, E. Heath, The removal of bisphenols and other contaminants of emerging concern by hydrodynamic cavitation: From lab-scale to pilot-scale, Sci. Total Environ. 743 (2020) 140724, https://doi.org/10.1016/j.scitotenv.2020.140724.
[41] R. Zhou, T. Zhang, R. Zhou, A. Mai-Prochnow, S.B. Ponraj, Z. Fang, H. Masood, J. Kananagh, D. McClure, D. Alam, K. (Ken) Ostrikov, P.J. Cullen, Underwater microplasma bubbles for efficient and simultaneous degradation of mixed dye pollutants, Science of the Total Environment 750 (2021) 142295. https://doi.org/10.1016/j.scitotenv.2020.142295.
[42] R. Zhou, R. Zhou, D. Alam, T. Zhang, W. Li, Y. Xia, A. Mai-Prochnow, H. An, E.C. Lovell, H. Masood, R. Amal, K. (Ken) Ostrikov, P.J. Cullen, Plasmacatalytic bubbles using CeO2 for organic pollutant degradation, Chemical Engineering Journal 403 (2021) 126413. https://doi.org/10.1016/j.cej.2020.126413.
[43] B. Maršálek, E. Maršálková, K. Odehnalová, F. Pochylý, P. Rudolf, P. Stahel, J. Rahel, J. Čech, S. Fialová, Š. Zezulka, Removal of Microcystis aeruginosa through the combined effect of plasma discharge and hydrodynamic cavitation, Water (switzerland) 12 (2020), https://doi.org/10.3390/w12010008.
[44] V.O. Abramov, A.V. Abramova, G. Cravotto, R.V. Nikonov, I.S. Fedulov, V. K. Ivanov, Flow-mode water treatment under simultaneous hydrodynamic cavitation and plasma, Ultrason Sonochem 70 (2021) 105323, https://doi.org/10.1016/j.ultsonch.2020.105323.
[45] A. Filipić, D. Dobnik, I. Gutiérrez-Aguirre, M. Ravnikar, T. Košir, Š. Baebler, A. Štern, B. Žegura, M. Petkovšek, M. Dular, M. Mozetič, R. Zaplotnik, G. Primc, Cold plasma within a stable supercavitation bubble – A breakthrough technology for efficient inactivation of viruses in water, Environ Int 182 (2023), https://doi.org/10.1016/j.envint.2023.108285.
[46] P. Rudolf, P. Stahel, B. Marsalek, J. Cech, J. Rahel, L. Prokes, E. Marsalkova, M. Balko, OP18: Synergistic effect of hydrodynamic cavitation and cold plasma discharge for water treatment and pollutants removal, in: ESS2022, 17th Meeting of the European Society of Sonochemistry, 2022: pp. 13–14.
[47] D. Podbevšek, G. Ledoux, M. Dular, Investigation of hydrodynamic cavitation induced reactive oxygen species production in microchannels via chemiluminescent luminol oxidation reactions, Water Res 220 (2022), https://doi.org/10.1016/j.watres.2022.118628.
[48] Primc G., Zaplotnik R., Mozetič M., FIilipić A., Guiterrez Aguirre I., Dobnik D., Dular M., Petkovšek M., Method and device for disinfection of liquid US11807555B2, USPTO, 2023 -10-18, EP3981743 (A1), 2022-04-13. EP3981743 (A1)., US11807555B2, 2020.
[49] U. Fantz, S. Briefi, D. Rauner, D. Wünderlich, Quantification of the VUV radiation in low pressure hydrogen and nitrogen plasmas, Plasma Sources Sci Technol 25 (2016), https://doi.org/10.1088/0963-0252/25/4/045006.
[50] D. Cecconet, J. Raček, A. Callegari, P. Hlavínek, Energy recovery from wastewater: A study on heating and cooling of a multipurpose building with sewage-reclaimed heat energy, Sustainability (switzerland) 12 (2020), https://doi.org/10.3390/su12010116.
[51] M. Cyprowski, A. Stobnicka-Kupiec, A. Ławniczek-Wałczyk, A. Bakal-Kijek, M. Gołofit-Szymczak, R.L. Górny, Anaerobic bacteria in wastewater treatment plant, Int Arch Occup Environ Health 91 (2018) 571–579, https://doi.org/10.1007/s00420-018-1307-6.
[52] M. Zupanc, T. Kosjek, M. Petkovšek, M. Dular, B. Kompare, B. Širok, M. Stražar, E. Heath, Shear-induced hydrodynamic cavitation as a tool for pharmaceutical micropollutants removal from urban wastewater, Ultrason Sonochem 21 (2014) 1213–1221, https://doi.org/10.1016/j.ultsonch.2013.10.025.
[53] G. Babu, P. Babu, M. Khagga, Preparation, characterization, and in vivo evaluation of valsartan porous matrices using emulsion solvent evaporation technique, Int J Pharm Investig 6 (2016) 169, https://doi.org/10.4103/2230-973x.187345.
[54] M. Zupanc, M. Petkovšek, J. Zevnik, G. Kozmus, A. Šmid, M. Dular, Anomalies detected during hydrodynamic cavitation when using salicylic acid dosimetry to measure radical production, Chem. Eng. J. 396 (2020), https://doi.org/10.1016/j.cej.2020.125389.
[55] J. Glienke, W. Schillberg, M. Stelter, P. Braeutigam, Prediction of degradability of micropollutants by sonolysis in water with QSPR - a case study on phenol derivates, Ultrason Sonochem 82 (2022), https://doi.org/10.1016/j.ultsonch.2021.105867.
[56] S. Sudhakaran, G.L. Amy, QSAR models for oxidation of organic micropollutants in water based on ozone and hydroxyl radical rate constants and their chemical classification, Water Res 47 (2013) 1111–1122, https://doi.org/10.1016/j.watres.2012.11.033.
[57] M.J. Lundqvist, L.A. Eriksson, Hydroxyl Radical Reactions with Phenol as a Model for Generation of Biologically Reactive Tyrosyl Radicals, J. Phys. Chem. B 104 (2000) 848–855, https://doi.org/10.1021/jp993011r.
[58] C.Y. Hu, Y.J. Liu, W.H. Kuan, Ph-dependent degradation of diclofenac by a tunnel-structured manganese oxide, Water (switzerland) 12 (2020), https://doi.org/10.3390/W12082203.
[59] J. De Boer, P. Garrigues, J.-D. Gu, K.C. Jones, T.P. Knepper, A. Newton, D.L. Sparks, The Handbook of Environmental Chemistry, n.d. http://www.springer.com/series/698.